nature geoscience

ARTICLES

https://doi.org/10.1038/s41561-019-0348-0

An isotopically depleted lower mantle component is intrinsic to the Hawaiian mantle plume

C. DeFelice[1*], S. Mallick[2], A. E. Saal[2] and S. Huang[1*]

Most ocean island basalts sample an isotopically depleted mantle component, but the origin of this component is unclear. It may come from either the entrained upper mantle or from a reservoir intrinsic to the plume, sourced from the lower mantle. For Hawaii, the isotopically depleted component is primarily sampled during the secondary rejuvenated-stage volcanism, 0.5–2 million years after the initial shield-stage volcanism. However, it is also inferred in shield and post-shield lavas. We analyse the radiogenic isotopic and trace element compositions of a suite of Mauna Kea shield-stage tholeiites, and found that they have the same isotopic compositions as rejuvenated-stage lavas. We use trace element models to show that these shield-stage basalts can be explained as higher degree partial melts of a rejuvenated-stage source. Our data, therefore, show that the depleted rejuvenated-stage component was directly sampled during shield-stage volcanism. The common source for both shield-stage and secondary rejuvenated volcanism implies that the depleted rejuvenated component is intrinsic to the Hawaiian mantle plume. It is further inferred that the mantle region from which the Hawaiian plume originates, probably in the lower mantle, is also isotopically depleted, similar but not identical to the upper mantle.

The compositions of ocean island basalts (OIBs) and mid-ocean ridge basalts (MORBs) reflect the compositional evolution of the Earth's interior. MORBs tend to have lower $^{87}Sr/^{86}Sr$ and higher $^{143}Nd/^{144}Nd$ and $^{176}Hf/^{177}Hf$ in comparison to OIBs. MORBs sample the upper mantle, which is 'depleted'[1] in highly incompatible trace elements. OIBs, such as those from Hawaii, Iceland, Samoa, Galapagos and Kerguelen, have higher $^{87}Sr/^{86}Sr$ and lower $^{143}Nd/^{144}Nd$ and $^{176}Hf/^{177}Hf$, which are described as isotopically 'enriched'. Pb isotope ratios ($^{206,207,208}Pb/^{204}Pb$) are more complicated; although many OIB values overlap with MORB values, OIBs range to more radiogenic Pb isotopes. Some OIBs are produced by mantle plumes from the lower mantle[2–5] and provide a rare opportunity to investigate the composition of the lower mantle and the long-term geochemical differentiation of the Earth. Although the majority of OIBs have enriched isotopic and elemental characteristics relative to MORBs, many OIBs contain a distinct isotopically depleted component with low $^{87}Sr/^{86}Sr$ and high $^{143}Nd/^{144}Nd$ and $^{176}Hf/^{177}Hf$, for example, Hawaii[6–13], Iceland[14–16], Kerguelen[17,18], Samoa[19,20] and Galapagos[21–23].

Isotopically depleted components in OIBs

The origin of the isotopically depleted components in hotspots globally is contentious, but critical to understand the long-term evolution of the Earth's mantle. There are three main hypotheses: (1) the depleted source component is intrinsic to the plume[9–13], (2) entrained upper mantle[6–8] or (3) metasomatized lithospheric mantle[24,25]. These hypotheses can be distinguished by their Nd and Hf isotope ratios, because depleted plume components are expected to have distinct Nd–Hf isotopic signatures from the upper mantle sampled by MORBs[26]. All three models were suggested for Galapagos and Iceland[14–16,21–23,27,28], where the depleted components have been attributed to either the local lithospheric and upper mantle contributions or an intrinsic plume component. At Ninetyeast Ridge (Kerguelen) the depleted component is isotopically and chemically distinct from the Indian MORB, and probably intrinsic to the plume[18], whereas at Samoa the depleted component is thought to be entrained depleted mantle (DM)[20,29]. Understanding the isotopically depleted end members of hotspots is critical to understanding the long-term evolution of the Earth's mantle.

The origin of the isotopically depleted component at Hawaii is still under debate. At Hawaii, isotopically depleted lavas commonly erupt during rejuvenated-stage volcanism, 0.5–2 Myr after the end of the isotopically enriched shield-stage volcanism[30–33]. Rejuvenated-stage volcanism occurs on the islands of Kaula, Kauai, Niihau, Oahu, Molokai and Maui (Fig. 1). Lavas erupted off-axis of the plume, called the North and South Arch Volcanic Field, are also grouped with rejuvenated-stage lavas because they have similar radiogenic isotope ratios and trace element abundances. The cause of these eruptions is probably flexural arching of the lithosphere caused by the building of Hawaiian volcanoes[34,35]. The mantle source of Hawaiian rejuvenated-stage lavas may be the Pacific MORB source[6], local lithospheric mantle[7] and also an isotopically depleted intrinsic plume component[8–13,36–39].

The isotopically depleted rejuvenated-stage components were also inferred in lavas from the pre-shield stage of Loihi[13], the shield stage of Kauai[13,36] and the post-shield stages of Hualaiai[33] and Mahukona[33,37]. However, in these cases, it is debatable whether the depleted component sampled by these shield lavas is DM or a depleted plume component. For example, some Kauai shield lavas form a positive $^{206}Pb/^{204}Pb$ versus $^{87}Sr/^{86}Sr$ trend, which points to the rejuvenated-stage lava field or MORB field (see Fig. 8 of Mukhopadhyay et al.[13]). However, Kauai shield lavas still have isotope ratios within the shield-stage range. Lavas from the Hana Volcanics of Haleakala have isotopic signatures similar to those of rejuvenated-stage lavas. However, it is debatable whether the Hana Volcanics belongs to post-shield-stage volcanism or rejuvenated-stage volcanism[40]. Nevertheless, post-shield and pre-shield volcanism sample the edge of the plume; consequently, it is difficult to unambiguously assess whether the depleted components sampled by the above-mentioned lavas are intrinsic to the Hawaiian plume.

The Emperor Seamounts, which were also created by the Hawaiian plume, contain an isotopically depleted component, similar to that sampled by Hawaiian rejuvenated-stage lavas[8,10]. Owing to

[1]University of Nevada, Las Vegas, Las Vegas, NV, USA. [2]Brown University, Providence, RI, USA. *e-mail: defelc1@unlv.nevada.edu; shichun.huang@unlv.edu

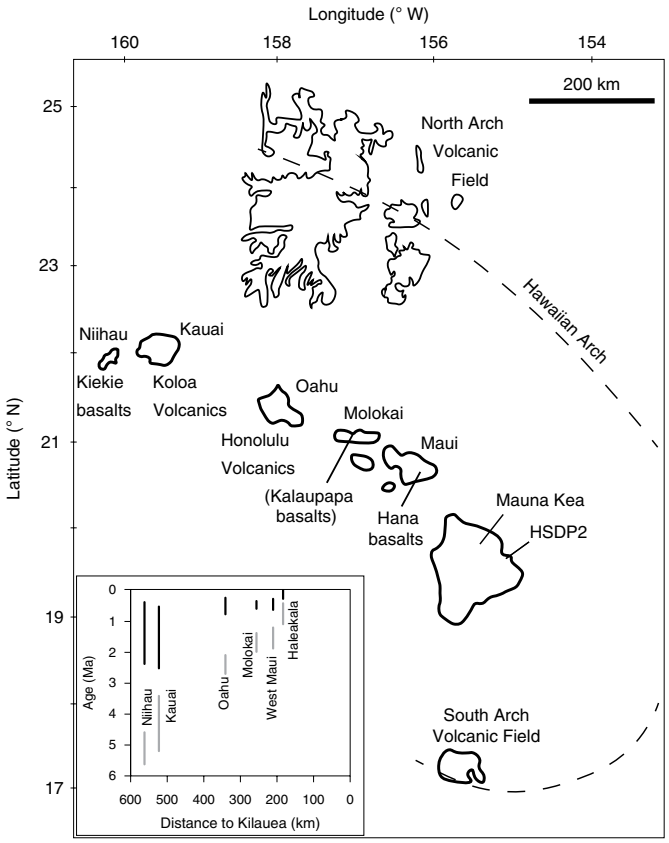

Fig. 1 | Map of the Hawaiian Islands and the Hawaiian Arch. Inset, Age and duration of rejuvenated-stage volcanism (black bars) and shield-stage volcanism (grey bars) at each respective island. Data are from Ozawa et al.[32]. The dashed line is the approximate trace of the Hawaiian Arch, a flexing of the lithosphere caused by the building of the Hawaiian volcanoes[34,35]. The label in brackets indicates a location not discussed in this study.

the proximity of the Hawaiian plume to a spreading centre when they formed, the Emperor Seamounts may sample the depleted upper mantle[6], although others argue that the depleted source component is intrinsic to the plume[8,10]. However, plume–ridge interaction cannot explain isotopically depleted Hawaiian rejuvenated-stage lavas in the middle of the Pacific plate, far removed from any spreading centre[41]. Hence, the location and nature of the isotopically depleted reservoir sampled by Hawaiian volcanism remains debated and critical to understanding the nature of the Hawaiian plume.

Depleted isotopic signature in Mauna Kea high-CaO lavas

In this study, we focus on lavas from 1,760–1,810 m.b.s.l. (meters below sea level) from the Hawaii Scientific Drilling Project (HSDP) that have elevated CaO (wt%) at a given MgO (wt%), which are referred to as high-CaO basalts[42–45] and are tholeiitic shield-stage lavas from Mauna Kea. HSDP cored 3.5 km of lavas from Mauna Kea volcano in Hilo, Hawaii, which represent ~500 kyr of volcanic growth[46]. A reference sample suite from the drill core[47] was investigated, which shows considerable variation in source composition and petrogenetic processes (Fig. 2). However, for the high-CaO basalts, major and trace element data exist only for seven glasses[42,45] and 24 whole rocks[44], and they are an important end member to understand the composition of the Hawaiian plume. Herzberg[43], for example, argued that the high-CaO basalts are the only true melts of peridotite and that most other Hawaiian basalts are the result of pyroxenite melting. Compared to other Mauna Kea shield tholeiites, the HSDP high-CaO basalts are enriched in the most and least incompatible elements, and their mantle source may be a mixed lithology of pyroxenite and peridotite[45].

Here we report Sr, Nd, Hf and Pb isotope ratios (Supplementary Table 1) and trace element concentrations (Supplementary Table 2) for 24 whole-rock high-CaO basalts that were previously analysed for their major and some trace element concentrations by X-ray fluorescence[44] (Supplementary Fig. 1). The high-CaO basalts have the most unradiogenic Pb and Sr isotopes and the most radiogenic Hf and Nd isotope ratios among the Hawaiian shield-stage lavas (Fig. 3). The high-CaO lavas have a higher ε_{Hf} at a given ε_{Nd} than modern Pacific MORBs and the estimated 100 million years old Pacific lithosphere (field outlined in Fig. 3c and details given in the Supplementary Information), suggesting that neither the local lithospheric mantle nor the Pacific mantle contribute to the high-CaO lavas (Fig. 3c).

These high-CaO lavas have the same Sr, Nd, Hf and Pb isotope compositions as the Hawaiian rejuvenated-stage alkalic lavas (Fig. 3), which shows that the depleted rejuvenated-stage component is also present during the Hawaiian shield-stage volcanism, in agreement with previous studies that have detected it in the pre-shield stage of Loihi[13], the shield stage of Kauai[13,36] and the post-shield stage of Hualaiai[33], Mahukona[33,37] and Haleakala[38]. Our high-precision Pb isotope data for high-CaO lavas fall on the same $^{206}Pb/^{204}Pb$ versus $^{208}Pb/^{204}Pb$ trends as those defined by lavas and high-pressure pyroxenite cumulates associated with the rejuvenated-stage Honolulu Volcanics on Oahu[9,11] (Fig. 4). This conclusion agrees with previous observations of heterogeneity within the depleted component[11,12,48] and reinforces the isotopic connection between the rejuvenated-stage component and Mauna Kea shield-stage high-CaO basalts.

Trace element evidence

With the isotopic similarity between high-CaO lavas and Hawaiian rejuvenated-stage lavas but their difference in major and trace element compositions, we hypothesized that HSDP tholeiitic high-CaO basalts represent high-degree partial melts of a depleted rejuvenated mantle source. That is, the rejuvenated-stage source component(s) was sampled by smaller degrees of partial melting during the Hawaiian rejuvenated-stage volcanism (to produce alkalic basalts) than the HSDP high-CaO lavas (tholeiitic basalts). To test this hypothesis, we used both non-modal fractional and batch melting models of the depleted rejuvenated-stage sources to reproduce their trace element patterns. Three groups of well-studied rejuvenated-stage lavas were used: Honolulu Volcanics[9] from Oahu, Kiekie basalts[12] from Niihau and lavas from the North Arch Volcanic Field[9]. A filter that excluded samples with MgO < 6.5 wt% was applied to avoid samples that crystallized more than just olivine. Data for samples with MgO > 6.5 wt% were then corrected to be in equilibrium with Fo_{90} to remove the olivine fractionation/accumulation effect. The source compositions were calculated assuming that rejuvenated-stage lavas are the products of low degrees of partial melting[9,30] (0.5–4.0%). The calculated source compositions were then melted to a higher degree[8] (6.0–9.5%) to see if they could reproduce the trace element patterns of the high-CaO basalts. The results of this model are shown in Fig. 5, and additional modelling details are given in the Supplementary Information. Our results show that the trace element patterns of the high-CaO basalts are consistent with those of high-degree partial melts of a rejuvenated-stage source. Our calculated depleted rejuvenated-stage source compositions are similar to those of the carbonatite-metasomatized source of Dixon et al.[12], who reconstructed the depleted rejuvenated-stage source compositions by metasomatizing a depleted peridotite with small amounts of incipient silicate or carbonatite melts[49] from the Hawaiian plume (Fig. 5d), a model first proposed by Chen and Frey[30] and also adopted here (Supplementary Fig. 4). Here we find that the same depleted component melted during the shield stage of volcanism.

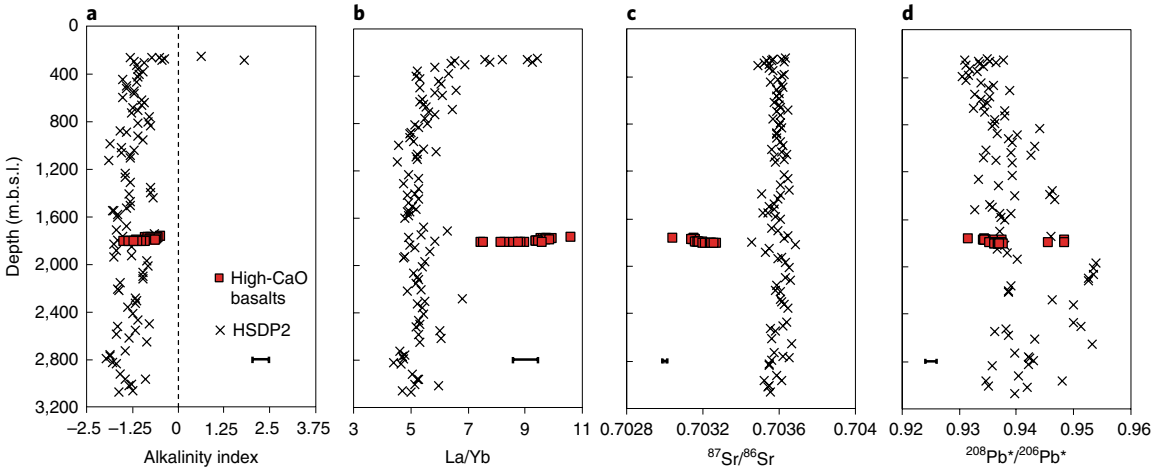

Fig. 2 | HSDP depth profiles. a–d, Depth profiles of the HSDP samples[44,61] versus the alkalinity index (**a**), La/Yb (**b**), $^{87}Sr/^{86}Sr$ (**c**) and $^{208}Pb^*/^{206}Pb^*$ (**d**). $Pb^* = (^{208}Pb/^{204}Pb_{sample} - ^{208}Pb/^{204}Pb_{CD})/(^{206}Pb/^{204}Pb_{sample} - ^{206}Pb/^{204}Pb_{CD})$, where CD refers to the values for the Canyon Diablo troilite. Rejuvenated-stage lavas are typically highly alkalic and occur to the right of the dashed line where alkalinity = 0 in **a**, whereas high-CaO basalts from the HSDP are tholeiitic basalts, left of the 0 line in **a**. Error bars represent the two standard error of measurements.

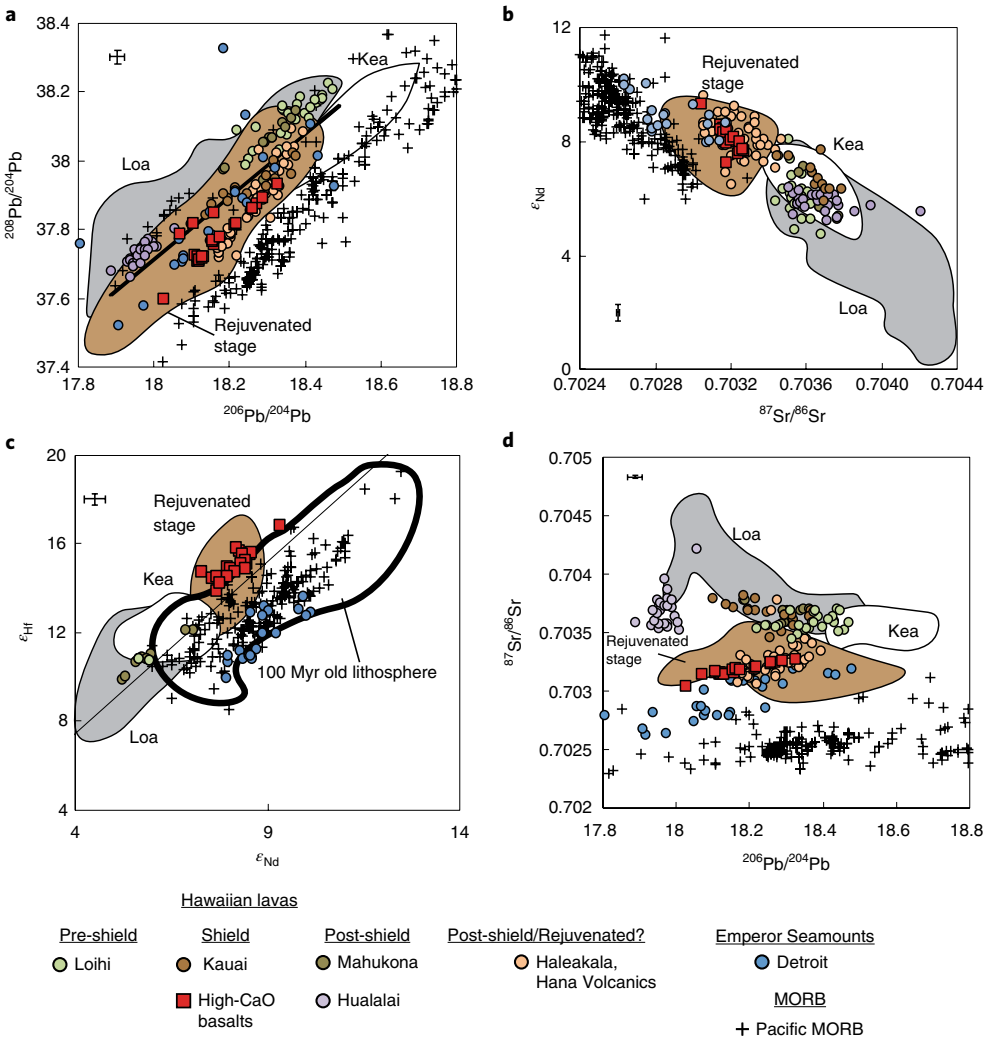

Fig. 3 | Radiogenic isotope data of Mauna Kea high-CaO basalts relative to shield-stage basalts of both Hawaiian Kea and Loa-trend volcanoes, rejuvenated-stage basalts and Pacific MORBs. a–d, $^{208}Pb/^{204}Pb$ versus $^{206}Pb/^{204}Pb$ (**a**), ε_{Nd} versus $^{87}Sr/^{86}Sr$ (**b**), ε_{Hf} versus ε_{Nd} (**c**) and $^{87}Sr/^{86}Sr$ versus $^{206}Pb/^{204}Pb$ (**d**). The thick line in **a** is the dividing line between Kea- and Loa-trend shield basalts[58]. The diagonal black line in **c** is the terrestrial array[62] and the field outlined with a thick black line in **c** is the calculated 100 Myr old lithosphere after MORB generation (Supplementary Information gives details). Error bars represent the two-standard error of measurements. Literature data sources are given in the Supplementary Information.

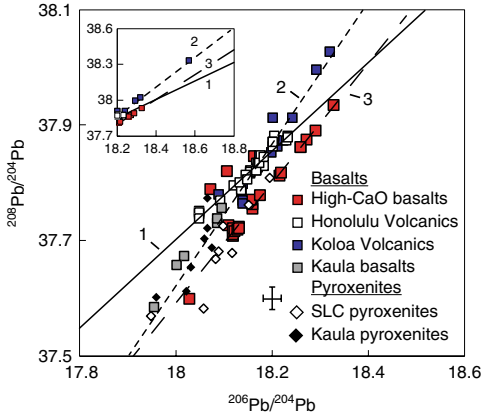

Fig. 4 | High-precision Pb isotope data for Hawaiian rejuvenated-stage lavas. The data are from the rejuvenated-stage basalts from Oahu (Honolulu Volcanics[39]), Kaula[11] and Koloa Volcanics on Kauai[36,48]. High-pressure pyroxenite cumulates are from Salt Lake Crater (SLC), which is associated with Honolulu Volcanics at Oahu[9,11] and Kaula[11]. Honolulu Volcanics define a slope of $y=0.7625\times+23.885$ that three high-CaO basalts fall on (line 1). High-CaO basalts also fall on line 3 defined by the SLC pyroxenites ($y=1.0338\times+18.983$). Koloa Volcanics define a slope ($y=1.2427\times+15.251$) that some Kaula pyroxenites and Kaula basalts fall on (line 2). Inset, Koloa Volcanics with more radiogenic Pb isotope ratios. Error bars are the two standard error of measurements.

DM[50] was also considered as a possible source, but we could not reproduce the trace element patterns of the high-CaO basalts by melting the DM. Specifically, partial melts of DM are too depleted in incompatible elements compared to high-CaO lavas (Supplementary Fig. 5). Compared to modern Pacific MORBs, the high-CaO lavas have a higher ε_{Hf} for a given ε_{Nd} (Fig. 3c), consistent with the inference that DM is not the source of the high-CaO lavas.

The depleted intrinsic plume component

We therefore conclude that the high-CaO basalts are high-degree partial melts of a rejuvenated source that is intrinsic to the Hawaiian plume, consistent with plume models of previous studies[8–13,34,35,51]. The Hawaiian mantle plume thus consists of enriched shield-stage components embedded as 'plums' inside a refractory matrix that is the source of depleted rejuvenated-stage lavas. During shield-stage volcanism, the enriched low-solidi shield-stage components start to melt first, and the refractory depleted component provides heat to enhance the melting of the enriched components[52,53]. Hence, partial melting of the refractory depleted component is limited and overwhelmed by partial melting of the enriched components during shield-stage volcanism.

Hawaiian rejuvenated-stage volcanism and arch volcanism are thought to be produced by flexural arc decompression melting[34,35]. Because of the volcanic loading, the Pacific plate is bent so that a flexural uplift of up to 100 m occurs at a distance of 200–400 km from the volcanic loading centre. This flexural uplift can produce a small degree of partial melting of the depleted component spread out beneath the lithosphere during shield-stage volcanism, which produces onshore rejuvenated-stage volcanism and offshore arch volcanism[34,35]. The enriched plume components are consumed during shield-stage volcanism, which allows the refractory depleted component to melt and produce isotopically depleted, highly alkalic lavas[18,34,35,51] during the rejuvenated-stage and arch volcanism.

In the case of the high-CaO basalts at Mauna Kea, it is possible that the portion of the plume that contributed to high-CaO lavas did not contain a significant amount of enriched shield components. That is, the mantle source of high-CaO basalts is dominated by the

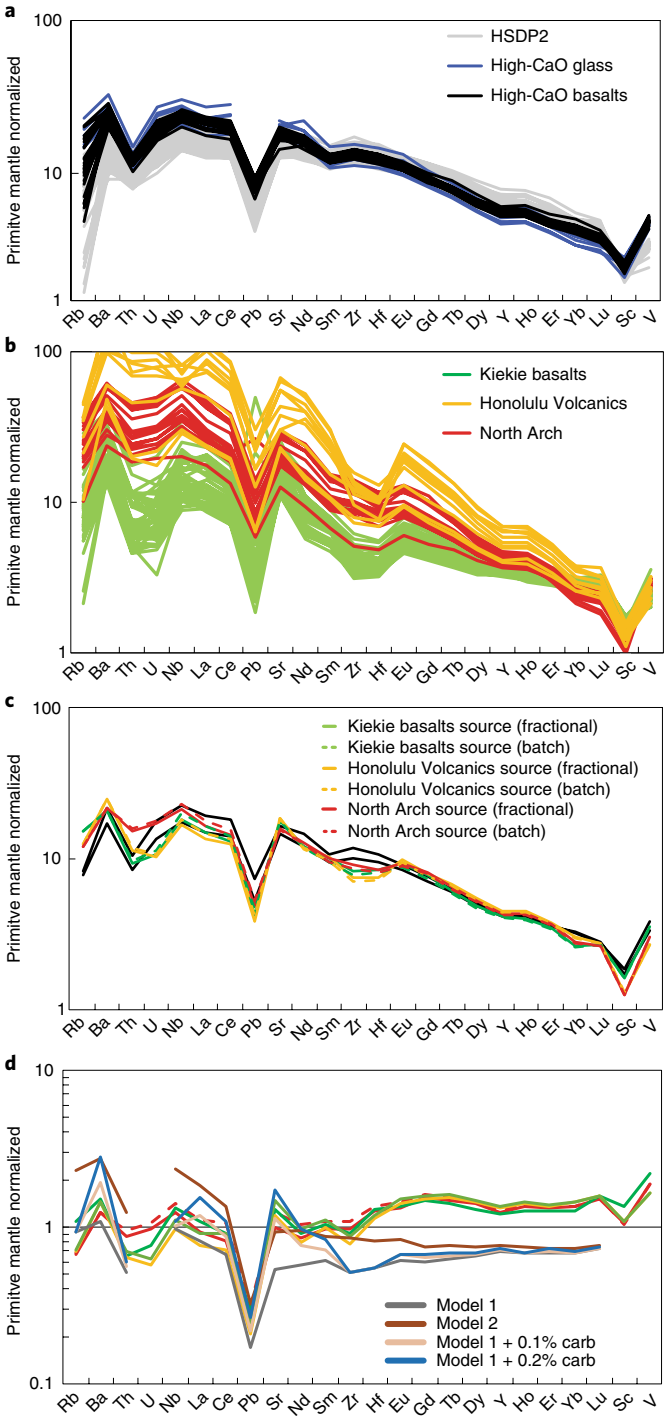

Fig. 5 | Trace element patterns and models. a, Primitive mantle-normalized trace element patterns for the HSDP reference suite samples (data references are in the Supplementary Information), high-CaO basalts (this study) and high-CaO glasses[42] corrected to Fo_{90} by adding or subtracting olivine. **b**, Rejuvenated-stage lavas from Honolulu Volcanics on Oahu, North Arch Volcanic Field and Kiekie basalts from Niihau, corrected to Fo_{90} by adding or subtracting olivine, used for the partial melting model. **c**, Results of our partial melting model relative to the range of values for high-CaO basalts enveloped by the two black lines. **d**, Calculated source compositions in this study (same key in **c**) compared to those of Dixon et al.[12] (key in **d**). 'Carb' in **d** is carbonatite[12]. The Supplementary Information give details and data sources.

depleted rejuvenated-stage component. Because of the higher temperature during the shield-stage volcanism, this refractory depleted component melted to a large degree and generated tholeiitic lavas with rejuvenated-stage isotopic signatures. In this case, we obtain a rare glimpse of the true isotopic composition and nature of the depleted component intrinsic to the Hawaiian plume.

The duration of high-CaO lavas is ~2,400 years according to the age-depth model of Bryce et al.[54]. Using a plume upwelling rate of ~30 cm yr^{-1} (ref. [54,55]), the estimated size of the geochemical heterogeneity is ~720 m. That is, the Hawaiian plume is heterogeneous at the subkilometre scale. For comparison, the radius of the magma capture zone at Hawaii is estimated to be 25–30 km (refs. [56,57]). Apparently, the compositions of erupted lavas reflect the sum of different plume components sampled by the melting events, and the short-scale source heterogeneity is homogenized to some degree during melting process[54,56]. The observed Loa-Kea geochemical difference[58–60] between the two Hawaiian volcanic trends must thus reflect the fact that their plume sources are more different than those shown in the lavas.

Online content

Any methods, additional references, Nature Research reporting summaries, source data, extended data, supplementary information, acknowledgements, peer review information; details of author contributions and competing interests; and statements of data and code availability are available at https://doi.org/10.1038/s41561-019-0348-0.

Received: 27 September 2018; Accepted: 6 March 2019;
Published online: 22 April 2019

References

1. Hofmann, A. W. Chemical differentiation of the Earth: the relationship between mantle, continental crust, and oceanic crust. *Earth Planet. Sci. Lett.* **90**, 297–314 (1988).
2. Kurz, M. D., Curtice, J., Lott, D. E. & Solow, A. Rapid helium isotopic variability in Mauna Kea shield lavas from the Hawaiian Scientific Drilling Project. *Geochem. Geophys. Geosys.* **5**, Q04G14 (2004).
3. DePaolo, D. J. & Wasserburg, G. J. Nd isotopic variations and petrogenetic models. *Geophys. Res. Lett.* **3**, 249–252 (1976).
4. Stracke, A. Earth's heterogeneous mantle: a product of convection-driven interaction between crust and mantle. *Chem. Geol.* **330–331**, 274–299 (2012).
5. Chen, C. Y. & Frey, F. A. Trace element and isotopic geochemistry of lavas from Haleakala volcano, East Maui, Hawaii: implications for the origin of Hawaiian basalts. *J. Geophys. Res.* **90**, 8743–8768 (1985).
6. Keller, R. A., Fisk, M. R. & White, W. M. Isotopic evidence for late Cretaceous plume–ridge interaction at the Hawaiian hotspot. *Nature* **405**, 673–676 (2000).
7. Lassiter, J. C., Hauri, E. H., Reiners, P. W. & Garcia, M. O. Generation of Hawaiian post-erosional lavas by melting of a mixed lherzolite/pyroxenite source. *Earth Planet. Sci. Lett.* **178**, 269–284 (2000).
8. Regelous, M., Hofmann, A. W., Abouchami, W. & Galer, S. J. G. Geochemistry of lavas from the Emperor Seamounts, and the geochemical evolution of Hawaiian magmatism from 85 to 42 Ma. *J. Petrol.* **44**, 113–140 (2003).
9. Yang, H. J., Frey, F. A. & Clague, D. A. Constraints on the source components of lavas forming the Hawaiian North Arch and Honolulu Volcanics. *J. Petrol.* **44**, 603–627 (2003).
10. Frey, F. A., Huang, S., Blichert-Toft, J., Regelous, M. & Boyet, M. Origin of depleted components in basalt related to the Hawaiian hot spot: evidence from isotopic and incompatible element ratios. *Geochem. Geophys. Geosys.* **6**, Q02L07 (2005).
11. Bizimis, M., Salters, V. J. M., Garcia, M. O. & Norman, M. D. The composition and distribution of the rejuvenated component across the Hawaiian plume: Hf–Nd–Sr–Pb isotope systematics of Kaula lavas and pyroxenite xenoliths. *Geochem. Geophys. Geosys.* **14**, 4458–4478 (2013).
12. Dixon, J., Clague, D. A., Cousens, B., Monsalve, M. L. & Uhl, J. Carbonatite and silicate melt metasomatism of the mantle surrounding the Hawaiian plume: evidence from volatiles, trace elements, and radiogenic isotopes in rejuvenated-stage lavas from Niihau, Hawaii. *Geochem. Geophys. Geosys.* **9**, Q09005 (2008).
13. Mukhopadhyay, S., Lassiter, J. C., Farley, K. A. & Bogue, S. W. Geochemistry of Kauai shield-stage lavas: implications for the chemical evolution of the Hawaiian plume. *Geochem. Geophys. Geosys.* **4**, 1009 (2003).
14. Chauvel, C. & Hémond, C. Melting of a complete section of recycled oceanic crust: trace element and Pb isotopic evidence from Iceland. *Geochem. Geophys. Geosys.* **1**, 1001 (2000).
15. Fitton, J., Saunders, A., Norry, M., Hardarson, B. & Taylor, R. Thermal and chemical structure of the Iceland plume. *Earth Planet. Sci. Lett.* **153**, 197–208 (1997).
16. Fitton, J. G., Saunders, A. D., Kempton, P. D. & Hardarson, B. S. Does depleted mantle form an intrinsic part of the Iceland plume? *Geochem. Geophys. Geosys.* **4**, 1032 (2003).
17. Storey, M. et al. Geochemical evidence for plume–mantle interactions beneath Kerguelen and Heard Islands, Indian Ocean. *Nature* **336**, 371–374 (1988).
18. Frey, F. A. et al. Depleted components in the source of hotspot magmas: evidence from the Ninetyeast Ridge (Kerguelen). *Earth Planet. Sci. Lett.* **426**, 293–304 (2015).
19. Jackson, M. G. et al. Helium and lead isotopes reveal the geochemical geometry of the Samoan plume. *Nature* **514**, 355–358 (2014).
20. Konter, J. G. & Jackson, M. G. Large volumes of rejuvenated volcanism in Samoa: evidence supporting a tectonic influence on late-stage volcanism. *Geochem. Geophys. Geosys.* **13**, Q0AM04 (2012).
21. Blichert-Toft, J. & White, W. M. Hf isotope geochemistry of the Galapagos Islands. *Geochem. Geophys. Geosys.* **2**, 2000GC000138 (2001).
22. Saal, A. E. et al. The role of lithospheric gabbros on the composition of Galapagos lavas. *Earth Planet. Sci. Lett.* **257**, 391–406 (2007).
23. Peterson, M. E. et al. Origin of the 'ghost plagioclase' signature in Galapagos melt inclusions: new evidence from Pb isotopes. *J. Petrol.* **55**, 2193–2216 (2014).
24. Pilet, S., Baker, M. B. & Stolper, E. M. Metasomatized lithosphere and the origin of alkaline lavas. *Science* **320**, 916–919 (2008).
25. Sorbadere, F., Médard, E., Laporte, D. & Schiano, P. Experimental melting of hydrous peridotite–pyroxenite mixed sources: constraints on the genesis of silica-undersaturated magmas beneath volcanic arcs. *Earth Planet. Sci. Lett.* **384**, 42–56 (2013).
26. Salters, V. J. M., Mallick, S., Hart, S. R., Langmuir, C. E. & Stracke, A. Domains of depleted mantle: new evidence from hafnium and neodymium isotopes. *Geochem. Geophys. Geosys.* **12**, Q08001 (2011).
27. Buchs, D. M., Hoernle, K., Hauff, F. & Baumgartner, P. O. Evidence from accreted seamounts for a depleted component in the early Galapagos plume. *Geology* **44**, 383–386 (2016).
28. Hanan, B. B., Blichert-Toft, J., Kingsley, R. & Schilling, J. G. Depleted Iceland mantle plume geochemical signature: artifact of multicomponent mixing? *Geochem. Geophys. Geosys.* **1**, 1003 (2000).
29. Workman, R. K. et al. Recycled metasomatized lithosphere as the origin of the Enriched Mantle II (EM2) end-member: evidence from the Samoan Volcanic Chain. *Geochem. Geophys. Geosys.* **5**, Q04008 (2004).
30. Chen, C. Y. & Frey, F. A. Origin of Hawaiian tholeiite and alkalic basalt. *Nature* **302**, 785–789 (1983).
31. Moore, J. G. & Clague, D. A. Volcano growth and evolution of the island of Hawaii. *Geol. Soc. Am. Bull.* **104**, 1471–1484 (1992).
32. Ozawa, A., Tagami, T. & Garcia, M. O. Unspiked K–Ar dating of the Honolulu rejuvenated and Ko'olau shield volcanism on O'ahu, Hawai'i. *Earth Planet. Sci. Lett.* **232**, 1–11 (2005).
33. Hanano, D., Weis, D., Scoates, J. S., Aciego, S. & DePaolo, D. J. Horizontal and vertical zoning of heterogeneities in the Hawaiian mantle plume from the geochemistry of consecutive postshield volcano pairs: Kohala-Mahukona and Mauna Kea-Hualalai. *Geochem. Geophys. Geosys.* **11**, Q01004 (2010).
34. Ribe, N. M. & Christensen, U. R. The dynamical origin of Hawaiian volcanism. *Earth Planet. Sci. Lett.* **171**, 517–531 (1999).
35. Bianco, T. A., Ito, G., Becker, J. M. & Garcia, M. O. Secondary Hawaiian volcanism formed by flexural arch decompression. *Geochem. Geophys. Geosys.* **6**, Q08009 (2005).
36. Garcia, M. O. et al. Petrology, geochemistry and geochronology of Kaua'i lavas over 4·5 Myr: implications for the origin of rejuvenated volcanism and the evolution of the Hawaiian plume. *J. Petrol.* **51**, 1507–1540 (2010).
37. Garcia, M. O. et al. Age, geology, geophysics, and geochemistry of Mahukona Volcano, Hawai'i. *Bull. Volcanol.* **74**, 1445–1463 (2012).
38. Phillips, E. H. et al. Isotopic constraints on the genesis and evolution of basanitic lavas at Haleakala, Island of Maui, Hawaii. *Geochim. Cosmochim. Acta* **195**, 201–225 (2016).
39. Fekiacova, Z., Abouchami, W., Galer, S. J. G., Garcia, M. O. & Hofmann, A. W. Origin and temporal evolution of Ko'olau Volcano, Hawai'i: inferences from isotope data on the Ko'olau Scientific Drilling Project (KSDP), the Honolulu Volcanics and ODP Site 843. *Earth Planet. Sci. Lett.* **261**, 65–83 (2007).
40. Sherrod, D. R., Nishimitsu, Y. & Tagami, T. New K–Ar ages and the geologic evidence against rejuvenated stage volcanism at Haleakalā, East Maui, a postshield-stage volcano of the Hawaiian island chain. *Bull. Geol. Soc. Am.* **115**, 683–694 (2003).

41. Huang, S., Regelous, M., Thordarson, T. & Frey, F. A. Petrogenesis of lavas from Detroit Seamount: geochemical differences between Emperor Chain and Hawaiian volcanoes. *Geochem. Geophys. Geosys.* **6**, Q01L06 (2005).
42. Stolper, E., Sherman, S., Garcia, M., Baker, M. & Seaman, C. Glass in the submarine section of the HSDP2 drill core, Hilo, Hawaii. *Geochem. Geophys. Geosys.* **5**, Q07G15 (2004).
43. Herzberg, C. Petrology and thermal structure of the Hawaiian plume from Mauna Kea volcano. *Nature* **444**, 605–609 (2006).
44. Rhodes, J. M., Huang, S., Frey, F. A., Pringle, M. & Xu, G. Compositional diversity of Mauna Kea shield lavas recovered by the Hawaii Scientific Drilling Project: inferences on source lithology, magma supply, and the role of multiple volcanoes. *Geochem. Geophys. Geosys.* **13**, Q03014 (2012).
45. Huang, S. & Humayun, M. Petrogenesis of high-CaO lavas from Mauna Kea, Hawaii: constraints from trace element abundances. *Geochim. Cosmochim. Acta* **185**, 198–215 (2016).
46. Sharp, W. D. & Renne, P. R. The $^{40}Ar/^{39}Ar$ dating of core recovered by the Hawaii Scientific Drilling Project (phase 2), Hilo, Hawaii. *Geochem. Geophys. Geosys.* **6**, Q04G17 (2005).
47. Rhodes, J. M. & Vollinger, M. J. Composition of basaltic lavas sampled by phase-2 of the Hawaii Scientific Drilling Project: geochemical stratigraphy and magma types. *Geochem. Geophys. Geosys.* **6**, Q03G13 (2004).
48. Garcia, M. O., Weis, D., Swinnard, L., Ito, G. & Pietruszka, A. J. Petrology and geochemistry of volcanic rocks from the South Kaua'i Swell Volcano, Hawai'i: implications for the lithology and composition of the Hawaiian Mantle Plume. *J. Petrol.* **56**, 1173–1197 (2015).
49. Dixon, J. E. et al. Light stable isotopic compositions of enriched mantle sources: resolving the dehydration paradox. *Geochem. Geophys. Geosys.* **18**, 3801–3839 (2017).
50. Salters, V. J. M. & Stracke, A. Composition of the depleted mantle. *Geochem. Geophys. Geosys.* **5**, Q05B07 (2004).
51. Phipps Morgan, J. Thermodynamics of pressure release melting of a veined plum pudding mantle. *Geochem. Geophys. Geosys.* **2**, 2000GC000049 (2001).
52. Brunelli, D., Cipriani, A. & Bonatti, E. Thermal effects of pyroxenites on mantle melting below mid-ocean ridges. *Nat. Geosci.* **11**, 520–525 (2018).
53. Jones, T. D. et al. The concurrent emergence and causes of double volcanic hotspot tracks on the Pacific plate. *Nature* **545**, 472–476 (2017).
54. Bryce, J. G., DePaolo, D. J. & Lassiter, J. C. Geochemical structure of the Hawaiian plume: Sr, Nd, and Os isotopes in the 2.8 km HSDP-2 section of Mauna Kea volcano. *Geochem. Geophys. Geosys.* **6**, Q09G18 (2005).
55. Farnetani, C. G., Hofmann, A. W. & Class, C. How double volcanic chains sample geochemical anomalies from the lowermost mantle. *Earth Planet. Sci. Lett.* **359–360**, 240–247 (2012).
56. DePaolo, D. J., Bryce, J. G., Dodson, A., Shuster, D. L. & Kennedy, B. M. Isotopic evolution of Mauna Loa and the chemical structure of the Hawaiian plume. *Geochem. Geophys. Geosys.* **2**, 2000GC000139 (2001).
57. Huang, S., Blichert-Toft, J., Fodor, R. V., Bauer, G. R. & Bizimis, M. Sr, Nd, Hf and Pb isotope systematics of postshield-stage lavas at Kahoolawe, Hawaii. *Chem. Geol.* **360–361**, 159–172 (2013).
58. Abouchami, W. et al. Lead isotopes reveal bilateral asymmetry and vertical continuity in the Hawaiian mantle plume. *Nature* **434**, 851–856 (2005).
59. Huang, S., Hall, P. S. & Jackson, M. G. Geochemical zoning of volcanic chains associated with Pacific hotspots. *Nat. Geosci.* **4**, 874–878 (2011).
60. Weis, D., Garcia, M. O., Rhodes, J. M., Jellinek, M. & Scoates, J. S. Role of the deep mantle in generating the compositional asymmetry of the Hawaiian mantle plume. *Nat. Geosci.* **4**, 831–838 (2011).
61. Huang, S. & Frey, F. A. Trace element abundances of Mauna Kea basalt from phase 2 of the Hawaii Scientific Drilling Project: petrogenetic implications of correlations with major element content and isotopic ratios. *Geochem. Geophys. Geosys.* **4**, 8711 (2003).
62. Vervoort, J. D., Plank, T. & Prytulak, J. The Hf–Nd isotopic composition of marine sediments. *Geochim. Cosmochim. Acta* **75**, 5903–5926 (2011).

Acknowledgements

This project was supported by NSF grants EAR-1524387 and NSF Ocean Sciences grant no. 1355932. C.D. acknowledges the UNLV Department of Geoscience for support through the Jack and Fay Ross fellowship.

Author contributions

C.D. and S.M. were responsible for the geochemical and isotopic measurements. All of the authors contributed to the data interpretation and model calculations and wrote the paper.

Competing interests

The authors declare no competing interests.

Additional information

Supplementary information is available for this paper at https://doi.org/10.1038/s41561-019-0348-0.

Reprints and permissions information is available at www.nature.com/reprints.

Correspondence and requests for materials should be addressed to C.D. or S.H.

Publisher's note: Springer Nature remains neutral with regard to jurisdictional claims in published maps and institutional affiliations.

Methods

Data compilation. All the geochemical data for the Hawaiian shield-stage[5,10,13,30,36,37,48,58,63–112] and rejuvenated-stage lavas[7,9,11,12,38,39,113–115] were collected from GEOROC (http://georoc.mpch-mainz.gwdg.de/georoc/) and compiled. Pacific MORB radiogenic isotope data were collected from the Geochemical Earth Reference Model (GERM) database (https://earthref.org/GERM/) on 24 January 2018 and compiled[116–139]. The search parameters set using the GERM database were the tectonic setting to spreading centres between 31.11 °N, 68.11 °S, 211.82 °W and 77.52° E. Sample types included were glass or whole-rock analyses of volcanic origin, classified as a basalt with major oxides, rare earth elements, trace elements or isotopic ratio data. The trace element data for rejuvenated-stage lavas used in the model were collected from GEOROC. North Arch Volcanic Field data are from Yang et al.[9] and Clague et al.[140] and those for Honolulu Volcanics are from Fekiacova et al.[39] and Clague and Frey[141], and for Kiekie basalts from Dixon et al.[12].

Sample preparation. Millipore ultrapure water (resistivity = 18 MΩ), double distilled acids using a subboiling PFA distiller and Baseline/Optima grade acids were used for the sample preparation.

Trace element analytical procedure. Trace element data for high-CaO basalts are reported in Supplementary Table 2. The sample of rock powder (~50 mg) was dissolved in acid-cleaned Savillex beakers using 3 ml of a 1:1 mix of HF:HNO_3 and placed on a hot plate for 2 wk at 100 °C. Samples were then dried down and rehydrated with 1 ml of 50% HNO_3 (by mass) and dried back down three separate times. Then, 6 ml of 50% HNO_3 was added to each sample and no undissolved residue was observed. An aliquot (2 ml) of each sample solution was pipetted into acid-cleaned 125 ml plastic bottles, in which the sample was diluted with 2% HNO_3 to a dilution factor of ~5,000. The samples were analysed for major and trace elements using a Thermo Scientific iCAP-Q inductively coupled plasma mass spectrometer (ICP-MS) at the University of Nevada, Las Vegas (UNLV) in kinetic energy discrimination (KED) mode to reduce polyatomic interferences. A typical analytical procedure of drift monitor–standard–unknown–unknown–unknown–unknown–drift monitor was used to monitor the sensitivity drift during analysis[61]. Three USGS rock standards were used, BHVO-1, BCR-1 and AGV-1, to produce linear calibration curves and BHVO-2 was measured as an unknown sample for quality control. For the elements that were measured by both UNLV ICP-MS and UMass X-ray fluorescence, data were compared, and our data agree with published data from the UMass XRF Lab[44] (Supplementary Fig. 2).

Radiogenic isotope analytical procedure. Sr, Nd, Hf and Pb were purified using ion exchange chromatography techniques. Sample dissolution and purification were performed in the PicoTrace clean lab at Brown University. About 500 mg of whole-rock powders were acid leached following the technique of Huang et al.[41] using 6 N double distilled HCl in an ultrasonic bath for 30 min. The acid was changed until the leachate was clear or pale yellow. Then, the samples were rinsed twice by adding Millipore water and sonicating for 30 min. Samples were then dried. About 100 mg of acid-leached sample was dissolved in a 3:1 HF:HNO_3 mixture following the procedure described above. Interested elements were extracted from the same sample aliquot in the order Pb, Hf, Sr/Nd (Supplementary Fig. 3). Pb was extracted first using AG1-X8 resin (100–200 mesh (BIO-RAD)). The matrix that remained from the Pb column was used to purify the remaining elements. First, Hf was removed from the matrix using Ln resin (Eichrom). Rb–Sr–REEs (rare earth elements) cut from the Hf column went through TRU-spec resin (Eichrom) to separate Rb–Sr from the REEs. The Rb–Sr cut from the TRU-spec resin then went through Sr-spec resin to separate Sr from Rb. The remaining matrix from the TRU-spec column that contained REEs was passed through Ln-spec resin to purify Nd. A schematic diagram (Supplementary Fig. 3) illustrates the order in which the columns were processed.

Sr, Nd, Hf and Pb isotope measurements were done at the Mass Spectrometer Analytical Facility at Brown University using a Thermo Scientific NEPTUNE PLUS multicollector ICP-MS. Sr, Nd and Hf were introduced to the plasma using a PFA nebulizer at a rate of ~70 µl min^{-1} coupled with a glass spray chamber. Pb was introduced to the plasma using an APEX-IR introduction system to enhance the sensitivity. The instrument was equipped with an H-skimmer cone and H-sampler cone. The baseline measurement was taken off peaks at -0.5 AMU. $^{87}Sr/^{86}Sr$, $^{143}Nd/^{144}Nd$ and $^{176}Hf/^{177}Hf$ were corrected for instrumental mass fractionation using $^{88}Sr/^{86}Sr = 0.1194$, $^{146}Nd/^{144}Nd = 0.7219$ and $^{179}Hf/^{177}Hf = 0.7325$ with the exponential law. The Pb solution was spiked with the NBS SRM-997 Tl standard prior to analysis with a Pb/Tl = 4 to correct for the instrumental mass fractionation using the exponential law with $^{203}Tl/^{205}Tl = 0.418922$. Sr, Nd and Hf were measured at 200 ppb concentration, whereas Pb was measured at a 75 ppb concentration level. $^{87}Sr/^{86}Sr$, $^{143}Nd/^{144}Nd$ and $^{176}Hf/^{177}Hf$ of the samples are reported relative to NBS SRM 987 $^{87}Sr/^{86}Sr = 0.71024$, the JNd-i Nd standard $^{143}Nd/^{144}Nd = 0.512115$ and the JMC-475 Hf standard $^{176}Hf/^{177}Hf = 0.282160$. $^{206}Pb/^{204}Pb$, $^{207}Pb/^{204}Pb$ and $^{208}Pb/^{204}Pb$ are reported relative to the NBS 981 standards $^{206}Pb/^{204}Pb = 16.9409$, $^{207}Pb/^{204}Pb = 15.4985$ and $^{208}Pb/^{204}Pb = 36.7222$ (ref. [142]). The external precision on the ratios over the course of two years is 30 ppm for Sr (2σ, $n = 75$) and Nd (2σ, $n = 104$), 40 ppm for Hf (2σ, $n = 89$) and 45–80 ppm for Pb (2σ, $n = 75$). The Sr and Pb blanks were <50 pg, and the Nd and Hf blanks were <30 pg. To ensure accuracy, three high-CaO basalt samples and two other HSDP samples that were studied previously[63,65–67] were dissolved again and the same procedure as described above was followed in a blind test in which the origins of the samples being processed were unknown until after they were measured. These values are reported in Supplementary Table 3 and compared with the original measurements. Duplicated samples agree with original values within the 2-standard error of their measurements (Supplementary Table 3).

Calculation for a 100 Myr old lithosphere. To calculate the isotopic composition of a 100 Ma lithosphere after MORB generation, we first calculated the Nd–Hf isotopic compositions of the DM at 100 Ma using present-day Nd–Hf isotopic compositions of MORB (references are in the data compilation above), and Sm/Nd and Lu/Hf of DM[50]. Then, the parent/daughter ratios (Sm/Nd and Lu/Hf) of the melting residue after MORB generation were calculated using partition coefficients given in Dixon et al.[12] and assuming a degree of partial melting of 10%. It was assumed that the melting residue retains 4% melt due to porosity (outer border of the field in Fig. 3c). A second field was calculated with 8% partial melting and 4% melt retained, but their values are close to those of the first calculation and almost overlap (inner border of the field in Fig. 3c). The retained melt is consistent with previous interpretations of a recently metasomatized depleted source for the rejuvenated-stage[9–12]. Then, we used the calculated Sm/Nd and Lu/Hf in the melting residue and the calculated DM Nd–Hf isotopic compositions at 100 Ma to calculate their present-day Nd–Hf isotopic compositions, which are plotted as fields in Fig. 3c.

Partial melting models. To test whether or not high-CaO trace element patterns can be produced by higher degrees of partial melting of a rejuvenated source, we calculated rejuvenated-stage source compositions and melted them to a higher degree. In detail, rejuvenated-stage lavas filtered for MgO > 6.5 wt% from the North Arch Volcanic Field, Honolulu Volcanics on Oahu and Kiekie basalts from Niihau were selected for this model because they have complete major and trace element data[9,11,12,140,141]. Their major and trace elements were corrected to be in equilibrium with Fo_{90} by adding or subtracting equilibrium olivine to the samples.

We back calculated their source compositions by using non-modal batch melting (equation (1)):

$$\frac{C_l}{C_o} = \frac{1}{D + F(1-P)} \quad (1)$$

where C_o is the initial source composition, C_l is the basalt composition normalized to Fo_{90}, D is the bulk partition coefficient and P is the bulk partition coefficient for the phases entering the melt (see Supplementary Table 4). The values for D and P are from refs. [12,45,61,143]. Equation (1) was rearranged to solve for the initial source composition (equation (2)):

$$C_o = C_l[D + F(1-P)] \quad (2)$$

The same method was applied using non-modal fractional melting and the source compositions back calculated by solving equation (3):

$$\frac{C_l}{C_o} = \frac{1}{F}\left[1-\left(1-\frac{FP}{D}\right)^{\left(\frac{1}{P}\right)}\right] \quad (3)$$

Equation (3) was rearranged to solve for the initial source composition (equation (4)):

$$C_o = \frac{(C_l F)}{1-\left(1-\frac{(DF)}{P}\right)^{\left(\frac{1}{P}\right)}} \quad (4)$$

A 'mismatch value' was calculated by summing the absolute values of the log difference of each potential basalt composition to the average high-CaO basalt composition and taking the absolute value to assess the potential match. Lower 'mismatch' values indicate a better fit to the average primitive mantle-normalized value of the high-CaO basalts. The best fits from both batch and fractional melting were produced using the same starting compositions and the same F values for the source calculations and the melts of the calculated source (details about best fits are given below). Here we model the aggregated liquids of fractional melting, which produces results similar to batch melting. However, the calculated source compositions using batch melting and fractional melting for a single sample are slightly different (Fig. 5).

Best-fit sources for Honolulu Volcanics, North Arch and Kiekie basalts were chosen (Fig. 5c). Specifically, Honolulu Volcanics sample 69KAL-2 was used to calculate the rejuvenated mantle source with a partial melting degree of 3.5%. Then this calculated mantle source was melted by 6.0% to reproduce a trace element pattern that is similar to that observed in HSDP high-CaO lavas. Similarly, the HSDP high-CaO trace element pattern can also be reproduced by 6.0% partial melting of a mantle source calculated using North Arch sample 9-1 with a partial

melting degree of 3.0, and 6.5% partial melting of a mantle source calculated using Kiekie basalts sample T318-R19 with a partial melting degree of 3.5%. Comparisons of the calculated sources are shown in Fig. 5d. Fractional melting produces a similar result because the aggregated liquid produced from fractional melting closely resembles equilibrium batch melting with a different degree of partial melting. Major element compositions of high-CaO basalts agree with this interpretation; they are tholeiitic and have lower concentrations of Na_2O and K_2O than rejuvenated-stage lavas (Supplementary Fig. 2).

High-CaO basalts have Ba/Th and La/Yb values that are intermediate among all the rejuvenated-stage lavas and within the shield-stage field. Ba is mobile during alteration. High-CaO basalts have a loss on ignition up to 10% (ref. [44]), which makes it difficult to ascertain whether they are the result of incipient silicate metasomatism or carbonatite metasomatism, as shown in Fig. 12 of Dixon et al.[12] (Supplementary Fig. 4). Melting of a pure DM source[50] was also considered and is a poor fit (Supplementary Fig. 5). DM melts at higher degrees of partial melting do not reproduce the pattern of the high-CaO basalts.

Data availability

The authors declare that all the data supporting the findings of this study are available within the article and its Supplementary Information.

References

63. Abouchami, W., Galer, S. J. G. & Hofmann, A. W. High precision lead isotope systematics of lavas from the Hawaiian Scientific Drilling Project. *Chem. Geol.* **169**, 187–209 (2000).
64. Xu, G., Frey, F. A., Clague, D. A., Weis, D. & Beeson, M. H. East Molokai and other Kea-trend volcanoes: magmatic processes and sources as they migrate away from the Hawaiian hot spot. *Geochem. Geophys. Geosys.* **6**, Q05008 (2005).
65. Blichert-Toft, J., Frey, F. A. & Albarède, F. Hf isotope evidence for pelagic sediments in the source of Hawaiian basalts. *Science* **285**, 879–882 (1999).
66. Blichert-Toft, J. & Albarède, F. Hf isotopic compositions of the Hawaii Scientific Drilling Project core and the source mineralogy of Hawaiian basalts. *Geophys. Res. Lett.* **26**, 935–938 (1999).
67. Eisele, J., Abouchami, W., Galer, S. J. G. & Hofmann, A. W. The 320 kyr Pb isotope evolution of Mauna Kea lavas recorded in the HSDP-2 drill core. *Geochem. Geophys. Geosys.* **4**, 8710 (2003).
68. Blichert-Toft., J., Weis, D., Maerschalk, C., Agranier, A. & Albarède, F. Hawaiian hot spot dynamics as inferred from the Hf and Pb isotope evolution of Mauna Kea volcano. *Geochem. Geophys. Geosys.* **4**, 8710 (2003).
69. Bryce, J. G., DePaolo, D. J. & Lassiter, J. C. Geochemical structure of the Hawaiian plume: Sr, Nd, and Os isotopes in the 2.8 km HSDP-2 section of Mauna Kea volcano. *Geochem. Geophys. Geosys.* **6**, Q09G18 (2005).
70. Chen, C. Y., Frey, F. A. & Garcia, M. O. Evolution of alkalic lavas at Haleakala Volcano, east Maui, Hawaii—major, trace element and isotopic constraints. *Contrib. Mineral. Petrol.* **105**, 197–218 (1990).
71. Chen, C. Y., Frey, F. A., Garcia, M. O., Dalrymple, G. B. & Hart, S. R. The tholeiite to alkalic basalt transition at Haleakala Volcano, Maui, Hawaii. *Contrib. Mineral. Petrol.* **106**, 183–200 (1991).
72. Chen, C. Y., Frey, F. A., Rhodes, J. M. & Easton, R. M. Temporal geochemical evolution of Kilauea Volcano: comparison of Hilina and Puna basalt. *Geophys. Monogr. Ser.* **95**, 161–181 (1995).
73. Easton, R. & Garcia, M. Petrology of the Hilina formation, Kilauea Volcano, Hawai'i. *Bull. Volcanol.* **43**, 657–673 (1980).
74. Gaffney, A. M., Nelson, B. K. & Blichert-Toft, J. Geochemical constraints on the role of oceanic lithospere in intra-volcano heterogeneity at West Maui, Hawaii. *J. Petrol.* **45**, 1663–1687 (2004).
75. Gaffney, A. M., Nelson, B. K. & Blichert-Toft, J. Melting in the Hawaiian plume at 1–2 Ma as recorded at Maui Nui: the role of eclogite, peridotite, and source mixing. *Geochem. Geophys. Geosys.* **6**, Q10L11 (2005).
76. Garcia, M. O., Rhodes, J. M., Trusdell, F. A. & Pietruszka, A. J. Petrology of lavas from the Puu Oo eruption of Kilauea Volcano: III. The Kupaianaha episode (1986–1992). *Bull. Volcanol.* **58**, 359–379 (1996).
77. Garcia, M. O., Pietruszka, A. J., Rhodes, J. M. & Swanson, K. Magmatic processes during the prolonged Pu'u'O'o eruption of Kilauea Volcano, Hawaii. *J. Petrol.* **41**, 967–990 (2000).
78. Hofmann, A. W., Feigenson, M. D. & Raczek, I. Case studies on the origin of basalt: III. Petrogenesis of the Mauna Ulu eruption, Kilauea, 1969–1971. *Contrib. Mineral. Petrol.* **88**, 24–35 (1984).
79. Wright, T. L., Swanson, D. A. & Duffield, W. A. Chemical compositions of Kilauea east rift lava, 1968–1971. *J. Petrol.* **16**, 110–133 (1975).
80. Hofmann, A. W., Feigenson, M. D. & Raczek, I. Kohala revisited *Contrib. Mineral. Petrol.* **95**, 114–122 (1987).
81. Norman, M. D. & Garcia, M. O. Primitive magmas and source characteristics of the Hawaiian plume: petrology and geochemistry of shield picrites. *Earth Planet. Sci. Lett.* **168**, 27–44 (1999).
82. Pietruszka, A. J. & Garcia, M. O. A rapid fluctuation in the mantle source and melting history of Kilauea Volcano inferred from the geochemistry of its historical summit lavas (1790–1982). *J. Petrol.* **40**, 1321–1342 (1999).
83. Rhodes, J. M. Geochemical stratigraphy of lava flows sampled by the Hawaii Scientific Drilling Project. *J. Geophys. Res.* **101**, 11729–11746 (1996).
84. Rhodes, J. M. & Vollinger, M. J. Composition of basaltic lavas sampled by phase-2 of the Hawaii Scientific Drilling Project: geochemical stratigraphy and magma types. *Geochem. Geophys. Geosys.* **5**, Q03G13 (2004).
85. Sims, K. W. W. et al. Porosity of the melting zone and variations in the solid mantle upwelling rate beneath Hawaii: inferences from ^{238}U–^{230}Th–^{226}Ra and ^{235}U–^{231}Pa disequilibria. *Geochim. Cosmochim. Acta* **63**, 4119–4138 (1999).
86. Stille, P., Unruh, D. M. & Tatsumoto, M. Pb, Sr, Nd, and Hf isotopic constraints on the origin of Hawaiian basalts and evidence for a unique mantle source. *Geochim. Cosmochim. Acta* **50**, 2303–2319 (1986).
87. Tanaka, R., Makishima, A. & Nakamura, E. Hawaiian double volcanic chain triggered by an episodic involvement of recycled material: constraints from temporal Sr–Nd–Hf–Pb isotopic trend of the Loa-type volcanoes. *Earth Planet. Sci. Lett.* **265**, 450–465 (2008).
88. West, H. B., Gerlach, D. C., Leeman, W. P. & Garcia, M. O. Isotopic constraints on the origin of Hawaiian lavas from the Maui Volcanic Complex, Hawaii. *Nature* **330**, 216–220 (1987).
89. Xu, G. et al. Geochemical characteristics of West Molokai shield- and postshield-stage lavas: constraints on Hawaiian plume models. *Geochem. Geophys. Geosys.* **8**, Q08G21 (2007).
90. Basu, A. R. & Faggart, B. E. Temporal isotopic variations in the Hawaiian mantle plume: the Lanai anomaly, the Molokai Fracture Zone and a seawater-altered lithospheric component in Hawaiian volcanism. *Geophys. Monogr. Ser.* **95**, 149–159 (1995).
91. Leeman, W. P., Gerlach, D. C., Garcia, M. O. & West, H. B. Geochemical variations in lavas from Kahoolawe volcano, Hawaii: evidence for open system evolution of plume-derived magmas. *Contrib. Mineral. Petrol.* 116, 62–77 (1994).
92. Huang, S. et al. Enriched components in the Hawaiian plume: evidence from Kahoolawe volcano, Hawaii. *Geochem. Geophys. Geosys.* **6**, Q11006 (2005).
93. Huang, S. et al. Ancient carbonate sedimentary signature in the Hawaiian plume: evidence from Mahukona Volcano, Hawaii. *Geochem. Geophys. Geosys.* **10**, Q08002 (2009).
94. Valbracht, P. J., Staudigel, H., Honda, M., McDougall, I. & Davies, G. F. Isotopic tracing of volcanic source regions from Hawaii: decoupling of gaseous from lithophile magma components. *Earth Planet. Sci. Lett.* **144**, 185–198 (1996).
95. Clague, D. A. Hawaiian alkaline volcanism. *Geol. Soc.* **30**, 227–252 (1987).
96. Bennett, V. C., Esat, T. M. & Norman, M. D. Two mantle-plume components in Hawaiian picrites inferred from correlated Os–Pb isotopes. *Nature* **381**, 221–224 (1996).
97. Stracke, A., Salters, V. J. M. & Sims, K. W. W. Assessing the presence of garnet–pyroxenite in the mantle sources of basalts through combined hafnium–neodymium–thorium isotope systematics. *Geochem. Geophys. Geosys.* **1**, 1006 (2000).
98. Cousens, B. L., Clague, D. A. & Sharp, W. D. Chronology, chemistry, and origin of trachytes from Hualalai Volcano, Hawaii. *Geochem. Geophys. Geosys.* **4**, 1078 (2003).
99. Lassiter, J. C. & Hauri, E. H. Osmium-isotope variations in Hawaiian lavas: evidence for recycled oceanic lithosphere in the Hawaiian plume. *Earth Planet. Sci. Lett.* **164**, 483–496 (1998).
100. Garcia, M. O., Foss, D. J. P., West, H. B. & Mahoney, J. J. Geochemical and isotopic evolution of Loihi volcano, Hawaii. *J. Petrol.* **36**, 1647–1671 (1995).
101. Hauri, E. H., Lassiter, J. C. & DePaolo, D. J. Osmium isotope systematics of drilled lavas from Mauna Loa, Hawaii. *J. Geophys. Res. Solid Earth* **101**, 11793–11806 (1996).
102. Rhodes, J. M. & Hart, S. R. Episodic trace element and isotopic variations in historical Mauna Loa lavas: implications for magma and plume dynamics. *Geophys. Monogr. Ser.* **92**, 263–288 (1995).
103. Kurz, M. D., Kenna, T. C., Kammer, D. P., Rhodes, J. M. & Garcia, O. Isotopic evolution of Mauna Loa Volcano: a view from the submarine Southwest Rift Zone. *Geophys. Monogr. Ser.* **92**, 289–306 (1995).
104. Cohen, A. S., Keith O'Nions, R. & Kurz, M. D. Chemical and isotopic variations in Mauna Loa tholeiites. *Earth Planet. Sci. Lett.* **143**, 111–124 (1996).
105. Garcia, M. O., Ito, E., Eiler, J. M. & Pietruszka, A. J. Crustal contamination of Kilauea Volcano magmas revealed by oxygen isotope analyses of glass and olivine from Puu Oo eruption lavas. *J. Petrol.* **39**, 803–817 (1998).
106. Garcia, M. O., Jorgenson, B. A., Mahoney, J. J., Ito, E. & Irving, A. J. An evaluation of temporal geochemical evolution of Loihi summit lavas: results from Alvin submersible dives. *J. Geophys. Res.* **98**, 537–550 (1993).

107. Frey, F. A., Garcia, M. O. & Roden, M. F. Geochemical characteristics of Koolau Volcano: implications of intershield geochemical differences among Hawaiian volcanoes. *Geochim. Cosmochim. Acta* **58**, 1441–1462 (1994).
108. Roden, M. F., Trull, T., Hart, S. R. & Frey, F. A. New He, Nd, Pb, and Sr isotopic constraints on the constitution of the Hawaiian plume: results from Koolau Volcano, Oahu, Hawaii, USA. *Geochim. Cosmochim. Acta* **58**, 1431–1440 (1994).
109. Stille, P., Unruh, D. M. & Tatsumoto, M. Pb, Sr, Nd and Hf isotopic evidence of multiple sources for Oahu, Hawaii basalts. *Nature* **304**, 25–29 (1983).
110. Haskins, E. H. & Garcia, M. O. Scientific drilling reveals geochemical heterogeneity within the Ko'olau shield, Hawai'i. *Contrib. Mineral. Petrol.* **147**, 162–188 (2004).
111. Salters, V. J. M., Blichert-Toft, J., Fekiacova, Z., Sachi-Kocher, A. & Bizimis, M. Isotope and trace element evidence for depleted lithosphere in the source of enriched Ko'olau basalts. *Contrib. Mineral. Petrol.* **151**, 297–312 (2006).
112. Jackson, M. C., Frey, Fa, Garcia, M. O. & Wilmoth, R. A. Geology and geochemistry of basaltic lava flows and dykes from the Trans-Loolau tunnel, Oahu, Hawaii. *Bull. Volcanol.* **60**, 381–401 (1999).
113. Reiners, P. W. & Nelson, B. K. Temporal–compositional–isotopic trends in rejuvenated-stage magmas of Kauai, Hawaii, and implications for mantle melting processes. *Geochim. Cosmochim. Acta* **62**, 2347–2368 (1998).
114. Cousens, B. L. & Clague, D. A. Shield to rejuvenated-stage volcanism on Kauai and Niihau, Hawaiian Islands. *J. Petrol.* **56**, 1547–1584 (2014).
115. Clague, D. A. & Dalrymple, G. B. Age and petrology of alkalic postshield and rejuvenated-stage lava from Kauai, Hawaii. *Contrib. Mineral. Petrol.* **99**, 202–218 (1988).
116. Castillo, P. R., Natland, J. H., Niu, Y. & Lonsdale, P. F. Sr, Nd and Pb isotopic variation along the Pacific–Antarctic risecrest, 53–57° S: implications for the composition and dynamics of the South Pacific upper mantle. *Earth Planet. Sci. Lett.* **154**, 109–125 (1998).
117. Castillo, P. R. et al. Petrology and Sr, Nd, and Pb isotope geochemistry of mid-ocean ridge basalt glasses from the 11° 45′ N to 15° 00′ N segment of the East Pacific Rise. *Geochem. Geophys. Geosys.* **1**, 1011 (2000).
118. Chauvel, C. & Blichert-Toft, J. A hafnium isotope and trace element perspective on melting of the depleted mantle. *Earth Planet. Sci. Lett.* **190**, 137–151 (2001).
119. Niu, Y. L., Collerson, K. D., Batiza, R., Wendt, J. I. & Regelous, M. Origin of enriched-type mid-ocean ridge basalt at ridges far from mantle plumes: the East Pacific Rise at 11° 20′ N. *Geophys. Res. Earth* **104**, 7067–7087 (1999).
120. Sims, K. W. W. et al. Chemical and isotopic constraints on the generation and transport of magma beneath the East Pacific Rise. *Geochim. Cosmochim. Acta* **66**, 3481–3504 (2002).
121. Sims, K. W. W. et al. Aberrant youth: chemical and isotopic constraints on the origin of off-axis lavas from the East Pacific Rise, 9°–10° N. *Geochem. Geophys. Geosys.* **4**, 8621 (2003).
122. Wendt, J. I., Regelous, M., Niu, Y., Hékinian, R. & Collerson, K. D. Geochemistry of lavas from the Garrett Transform Fault: insights into mantle heterogeneity beneath the eastern Pacific. *Earth Planet. Sci. Lett.* **173**, 271–284 (1999).
123. Goss, A. R. et al. Geochemistry of lavas from the 2005–2006 eruption at the East Pacific Rise, 9°46′ N–9° 56′ N: implications for ridge crest plumbing and decadal changes in magma chamber compositions. *Geochem. Geophys. Geosys.* **11**, Q05T09 (2010).
124. Waters, C. L. et al. Sill to surface: linking young off-axis volcanism with subsurface melt at the overlapping spreading center at 9° 03′ N East Pacific Rise. *Earth Planet. Sci. Lett.* **369–370**, 59–70 (2013).
125. Hahm, D., Castillo, P. R. & Hilton, D. R. A deep mantle source for high $^{3}He/^{4}He$ ocean island basalts (OIB) inferred from Pacific near-ridge seamount lavas. *Geophys. Res. Lett.* **36**, L20316 (2009).
126. Hamelin, C., Dosso, L., Hanan, B., Barrat, J. A. & Ondréas, H. Sr–Nd–Hf isotopes along the Pacific Antarctic Ridge from 41 to 53° S. *Geophys. Res. Lett.* **37**, L10303 (2010).
127. Hamelin, C. et al. Geochemical portray of the Pacific Ridge: new isotopic data and statistical techniques. *Earth Planet. Sci. Lett.* **302**, 154–162 (2011).
128. Hanan, B. B. & Schilling, J. G. Easter Microplate evolution: Pb isotope evidence. *J. Geophys. Res.* **94**, 7432–7448 (1989).
129. Fontignie, D. & Schilling, J. G. $^{87}Sr^{86}Sr$ and REE variations along the Easter Microplate boundaries (south Pacific): application of multivariate statistical analyses to ridge segmentation. *Chem. Geol.* **89**, 209–241 (1991).
130. Kingsley, R. H., Blichert-Toft, J., Fontignie, D. & Schilling, J. G. Hafnium, neodymium, and strontium isotope and parent–daughter element systematics in basalts from the plume–ridge interaction system of the Salas y Gomez Seamount Chain and Easter Microplate. *Geochem. Geophys. Geosys.* **8**, Q04005 (2007).
131. Kempton, P. D. et al. Sr–Nd–Pb–Hf isotope results from ODP Leg 187: evidence for mantle dynamics of the Australian–Antarctic Discordance and origin of the Indian MORB source. *Geochem., Geophys., Geosys.* **3**, 1074 (2002).
132. Klein, E. M., Langmuir, C. H., Zindler, A., Staudigel, H. & Hamelin, B. Isotope evidence of a mantle convection boundary at the Australian–Antarctic Discordance. *Nature* **333**, 623–629 (1988).
133. Salters, V. J. M. The generation of mid-ocean ridge basalts from the Hf and Nd isotope perspective. *Earth Planet. Sci. Lett.* **141**, 109–123 (1996).
134. Mahoney, J. J., Storey, M., Duncan, R. A., Spencer, K. J. & Pringle, M. in *The Mesozoic Pacific: Geology, Tectonics, and Volcanism* (eds Pringle, M., Sager, W. W., Sliter, W. V. & Stein, S.) 233–261 (American Geophysical Union, 1993).
135. Hanan, B., Blichert-Toft, J., Pyle, D. & Christie, D. Contrasting origins of the upper mantle MORB source revealed by Hf and Pb isotopes from the Australian–Antarctic Discordance. *Geochim. Cosmochim. Acta* **68**, A553– (2004).
136. Niu, Y., Waggoner, D. G., Sinton, J. M. & Mahoney, J. J. Mantle source heterogeneity and melting processes beneath seafloor spreading centers: the East Pacific Rise, 18°–19° S. *J. Geophys. Res.* **101**, 27711–27733 (1996).
137. Nowell, G. M. et al. High precision Hf isotope measurements of MORB and OIB by thermal ionisation mass spectrometry: insights into the depleted mantle. *Chem. Geol.* **149**, 211–233 (1998).
138. Lawson, K., Searle, R. C., Pearce, J. A., Browning, P. & Kempton, P. Detailed volcanic geology of the MARNOK area, Mid-Atlantic Ridge north of Kane Transform. *Geol. Soc.* **118**, 61–102 (1996).
139. Pyle, D. G., Christie, D. M. & Mahoney, J. J. Resolving an isotopic boundary within the Australian–Antarctic Discordance. *Earth Planet. Sci. Lett.* **112**, 161–178 (1992).
140. Clague, D. A., Holcomb, R. T., Sinton, J. M., Detrick, R. S. & Torresan, M. E. Pliocene and Pleistocene alkalic flood basalts on the seafloor north of the Hawaiian islands. *Earth Planet. Sci. Lett.* **98**, 175–191 (1990).
141. Clague, D. A. & Frey, F. A. Petrology and trace element geochemistry of the Honolulu Volcanics, Oahu: implications for the oceanic mantle below Hawaii. *J. Petrol.* **23**, 447–504 (1982).
142. Klaver, M. et al. Temporal and spatial variations in provenance of Eastern Mediterranean Sea sediments: implications for Aegean and Aeolian arc volcanism. *Geochim. Cosmochim. Acta* **153**, 149–168 (2015).
143. Lee, C. T. A., Leeman, W. P., Canil, D. & Li, Z. X. A. Similar V/Sc systematics in MORB and arc basalts: implications for the oxygen fugacities of their mantle source regions. *J. Petrol.* **46**, 2313–2336 (2005).